

Send proofs to: J. Melendez

A LOW SOLAR OXYGEN ABUNDANCE FROM THE FIRST OVERTONE OH LINES

Jorge Meléndez¹

Caltech, Department of Astronomy, M/C 105-24, 1200 E. California Blvd, Pasadena, CA 91125

jorge@astro.caltech.edu

ABSTRACT

An extremely high-resolution ($> 10^5$) high-S/N ($> 10^3$) solar spectrum has been used to measure 15 very weak first overtone ($\Delta v = 2$) infrared OH lines, resulting in a low solar abundance of $A_O \approx 8.6$ when MARCS, 3D, and spatially and temporally averaged 3D model atmospheres are used. A higher abundance is obtained with Kurucz ($A_O \approx 8.7$) and Holweger & Müller ($A_O \approx 8.8$) model atmospheres. The low solar oxygen abundance obtained in this work is in good agreement with a recent 3D analysis of [O I], O I, OH fundamental ($\Delta v = 1$) vibration-rotation and OH pure rotation lines (Asplund et al. 2004). The present result brings further support for a low solar metallicity, and although using a low solar abundance with OPAL opacities ruins the agreement between the calculated and the helioseismic measurement of the depth of the solar convection zone, recent results from the OP project show that the opacities near the base of the solar convection zone are larger than previously thought, bringing further confidence for a low solar oxygen abundance.

Subject headings: Sun: abundances - Sun: photosphere

¹Affiliated with the Seminario Permanente de Astronomía y Ciencias Espaciales of the Universidad Nacional Mayor de San Marcos, Peru.

1. Introduction

For many years, the accepted solar oxygen abundance was $A_O^1 \approx 8.9$. This value was supported by the impressive agreement between the abundance obtained from the [O I] lines (Lambert 1978, $A_O = 8.92$ dex), and the pure rotation (Sauval et al. 1984, $A_O = 8.91$ dex) and fundamental vibration-rotation OH lines (Grevesse et al. 1984, $A_O = 8.93$ dex). That solar oxygen abundance ($A_O = 8.9$) is high when compared to the abundance of nearby young OB stars (e.g. Daflon et al. 2003, $A_O = 8.6-8.7$ dex). Considering that the Sun is about 4.6 Gyr old, its oxygen abundance is supposed to be lower or equal than the present day interstellar medium (ISM). The “high” ($A_O = 8.9$) solar oxygen abundance with respect to the ISM could be explained by recent infall of metal-poor material into the local ISM (Meyer et al. 1994) or by migration (Wielen et al. 1996) of the Sun from an inner (more metal-rich) birthplace in the Galaxy to its present position.

Another alternative is to invoke errors in the oxygen abundance derived in the Sun (or in OB stars). The solar oxygen abundance has been recently revised (Allende Prieto et al. 2001; Asplund et al. 2004; Allende Prieto et al. 2004; hereafter AP01, A04 and AP04, respectively), yielding an abundance about 0.2-0.3 dex lower than previous determinations (Sauval et al. 1984; Grevesse et al. 1984; Grevesse & Sauval 1998). Although this result solves the apparent oxygen overabundance of the Sun with respect to the local ISM, it poses a new problem. The computed base of the solar convective zone (using the low value of the solar oxygen abundance) is then shallower than the value obtained from helioseismology (Bahcall & Pinsonneault 2004; Bahcall et al. 2004a; Basu & Antia 2004, Turck-Chize et al. 2004). This new solar problem has been called by Bahcall et al. (2004b) “the convective zone problem”. Furthermore, when low solar abundances are employed, the computed sound speed radial profile disagrees with sound speeds determined from helioseismological observations (Bahcall et al. 2004a; Basu & Antia 2004, Turck-Chize et al. 2004). Therefore, it is important to verify the proposed low solar oxygen abundance with other spectral features.

In the most comprehensive study utilizing different set of lines available for oxygen abundance determination in the Sun, namely the [O I] ($0.6 \mu\text{m}$), O I ($0.6 - 0.9 \mu\text{m}$), fundamental ($\Delta v = 1$) vibration-rotation OH ($3-4 \mu\text{m}$), and pure rotation OH ($9-13 \mu\text{m}$) lines, A04 derived $A_O = 8.66 \pm 0.05$ dex by using a 3D hydrodynamical model of the solar atmosphere. The first overtone ($\Delta v = 2$) OH lines ($1.5-1.8 \mu\text{m}$) were probably not included in that work because they are so weak that it is very difficult to identify and measure these lines in the solar spectrum². Note that in a recent 3D NLTE analysis of center-to-limb observations

¹ $A_X \equiv \log (N_X/N_H) + 12$

² After receiving the first report from the referee, we noted that first overtone OH lines in the solar

of the O I infrared triplet ($0.777 \mu\text{m}$), AP04 have obtained $A_O = 8.70 \pm 0.04$ dex, this is somewhat higher than the abundance obtained from permitted lines by A04 ($A_O = 8.64$). Considering the uncertainties in the NLTE modeling, both results are equally plausible.

In this work we present measurements of extremely weak first overtone infrared OH lines, which we use for a new determination of the oxygen abundance in the Sun.

2. Observational Data

The solar spectrum we use was obtained with the 1-m FTS at the McMarth-Pierce telescope (Kitt Peak) by Wallace & Livingston (2003, hereafter WL03). The center-disk solar spectrum was obtained at very high spectral resolution ($R = 700\,000$), and corrected for telluric lines (WL03). A portion of this spectrum is shown in Fig. 1.

The S/N of the spectrum is very high, it typically ranges from 900 to 1700, with a mean value of $S/N = 1350$, as measured from 20 continuum regions in the H band ($1.5 - 1.8 \mu\text{m}$). This extremely low-noise spectrum allows the measurement of features as weak as a few 0.1% of the continuum.

The printed version of the solar atlas of WL03 provides identification for more than seventy OH lines of the $\Delta v = 2$ sequence, from the bands (2,0), (3,1), and (4,2). The solar atlas of WL03 provides also identification for some features that are blended with the infrared OH lines. For the less obvious blends, a line list of atomic and CN lines (Meléndez & Barbuy 1999) was employed to avoid OH lines that are severely blended. Also, a search for new OH features present in the solar spectrum was undertaken using the list of OH lines by Goldman et al. (1998, hereafter G98). After careful examination, only 13 of the OH lines identified by WL03 were selected as suitable for an abundance analysis; the other lines were discarded because of blending with known atomic or CN lines (blends with unidentified absorption features were also taken into account, considering only OH lines with $\text{FWHM}^3 = 0.245 \pm 0.025 \text{ \AA}$). Two additional infrared OH lines were identified in the process.

The equivalent widths of the OH lines are shown in Table 1, they were measured by fitting gaussian profiles with IRAF. The error in the measurement of these weak features is about 10-20 % (0.04-0.08 dex), as estimated from several trials using different continua.

spectrum were first analyzed by Bonnell & Bell (1993), in a paper on “The gravities of K giant stars determined from [O I] and OH features”

³Bonnell & Bell (1993) reported an average $\text{FWHM} = 0.093 \text{ cm}^{-1}$ for 18 OH solar lines of the $\Delta v = 2$ sequence. This is equivalent to $\text{FWHM} = 0.249 \text{ \AA}$, in excellent agreement with our results (0.245 \AA)

These errors are consistent with an estimate obtained by using Cayrel's (1988) formula (7), that results in $\delta W_\lambda = 0.11 \text{ m}\text{\AA}$, which for a typical 1-m \AA OH line corresponds to an error of 0.045 dex.

The errors in W_λ could be also estimated from a comparison with measurements by Bonnell & Bell (1993), who used the infrared solar spectrum of Delbouille & Roland (1981), that has a lower spectral resolution by a factor of 2.33, but with higher S/N by a factor of 2.96, therefore both spectra have similar figure of merit $F \equiv (R \times [S/N])/\lambda$ (Norris et al. 2001), although note that the Delbouille & Roland solar atlas is not corrected of telluric blends. Bonnell & Bell (1993) give W_λ for 18 first-overtone OH lines in the H band, and eight of them are in common with our work. They estimated an uncertainty of 9% (0.04 dex) for their measurements, but the standard deviation of the oxygen abundance obtained by them is 0.09 dex (23%), therefore the errors of their W_λ are probably similar to our measurements (10-20%). A comparison for the eight OH lines in common is shown in Fig. 2. The mean difference (this work - theirs) is 0.07 m \AA ($\sigma = 0.19 \text{ m}\text{\AA}$), equivalent to a mean difference of 8% ($\sigma = 21\%$), or 0.03 dex ($\sigma = 0.08 \text{ dex}$).

3. Analysis

The list of OH lines and their molecular parameters has been previously described in Meléndez et al. (2001). It has been employed to determine the oxygen abundance in halo (Meléndez et al. 2001) and bulge stars (Meléndez et al. 2003). The gf -values of the first overtone OH vibration-rotation lines ($X^2\Pi$) were computed from the Einstein A coefficients given by G98, that are the most accurate available in the literature. Moreover, the transition probabilities of G98 are in good agreement with previous research (e.g. Holtzclaw et al. 1993), although significant differences exist with respect to the earliest works (e.g. Mies 1974). G98 and Holtzclaw et al. (1993) determined Einstein A coefficients employing the experimentally derived dipole moment function (DMF) by Nelson et al. (1990, hereafter N90). N90 also determined A coefficients, but only for OH lines with low J ($J'' \leq 14.5$) numbers (calculations for somewhat higher J numbers were made available by D. D. Nelson, Jr. 1999, private communication). Holtzclaw et al. (1993) noted that for lines of high J (and high v), an extrapolation of Nelson's DMF was necessary, although for the lines used in the present work the differences due to this extrapolation are negligible. In a different approach, G98 used a theoretical DMF outside the range of validity of Nelson's DMF, this allowed G98 to extend the calculation of Einstein coefficients to lines with very high J and v . Note, however, that for the typical first overtone OH lines observed in the solar spectrum (low v and J), any of these approaches give essentially the same result. G98 provides a

comparison with the values obtained by Holtzclaw and collaborators, and the agreement is excellent. In Fig. 3c it is shown the difference between the $\log gf$ value obtained by G98 and N90; the error bars were derived by N90, estimating the 95% confidence limit in its experimental DMF, taking into account both random and potential systematic errors. For the lines employed here, the error in the gf -values is about 0.03 dex.

Line positions and excitation potentials are from G98, they were calculated using the best available laboratory molecular constants, and the line positions were checked with laboratory wavenumbers (G98). The adopted value for the dissociation potential is 4.392 eV (Huber & Herzberg 1979). The parameters (wavelength, excitation potential, gf -value, quantum numbers) of the set of lines used in this work are giving in Table 1.

The oxygen abundance was obtained using the 2002 version of the program MOOG (Sneden 1973) and four model atmospheres: (i) a Kurucz model⁴ including convective overshooting, although a model with no overshooting (NOVER, Castelli & Kurucz 2004) was also used, but the difference in the oxygen abundance is only 0.01 dex (lower with the NOVER model); (ii) the temporally and spatially averaged 3D solar model⁵ (hereafter $\langle 3D \rangle$ model) by A04; (iii) a MARCS solar model (Asplund et al. 1997), (iv) the Holweger & Müller (1974, hereafter HM74) model atmosphere. Additionally, M. Asplund (private communication, 2004) have kindly made 3D calculations for a subset of the OH lines.

A microturbulence of 1 km s⁻¹ was adopted for the 1D modeling, yet the lines are so weak that the results do not depend on the adopted microturbulence. The calculations were done in LTE; this seem to be a good approximation for vibration-rotation OH lines (Hinkle & Lambert 1975).

The resulting abundances obtained with the $\langle 3D \rangle$ model are shown in Fig. 4 as a function of excitation potential, reduced equivalent width (W_λ/λ) and wavelength. As can be seen, the derived oxygen abundances show no trends with either excitation potential or wavelength. There is an apparent slight trend with reduced equivalent width, but within the measurement errors (§2) this is not significant. The use of other model atmospheres result in similar plots.

The mean value obtained from the 15 OH lines and the $\langle 3D \rangle$ model is $A_O = 8.59$ dex ($\sigma = 0.06$ dex). Full 3D calculations were kindly performed by M. Asplund for 5 lines of the $\Delta v = 2$ sequence with $\chi_{exc} = 0.30 - 1.24$ eV. After rescaling his results for the 15 OH lines, the full 3D result is 0.02 dex lower than the abundance obtained with the

⁴<http://kurucz.harvard.edu>

⁵The use of this model was suggested by the referee

<3D> model. The MARCS, Kurucz and HM74 models, give $A_O = 8.61$, 8.71 and 8.80 dex, respectively. Our results are in good agreement (except the result with the HM74 model) with 3D hydrodynamical simulations of other spectral features by AP01, A04 and AP04, who derived $A_O = 8.69 \pm 0.05$ dex, 8.66 ± 0.05 dex, and 8.70 ± 0.04 dex, respectively.

The main uncertainty in our results is the statistical error, due to the weakness of the OH lines. The only previous abundance analysis of the $\Delta v = 2$ sequence was performed by Bonnell & Bell (1993). They analyzed these lines in order to check the accuracy of the oscillator strengths, by comparing the abundance obtained with these lines and the OH lines of the $\Delta v = 1$ sequence. Bonnell & Bell (1993) used the HM74 model atmosphere and obtained an abundance of $A_O = 8.76$ ($\sigma = 0.09$ dex) with the first overtone vibration-rotation OH lines, that is 0.12 lower than the value they found with the fundamental OH lines. After considering the mean difference in gf -values and equivalent widths with respect to our work, their result is $A_O = 8.71 \pm 0.09$ dex, which is lower than the abundance we found with the HM74 model atmosphere ($A_O = 8.80$ dex ± 0.06 dex). M. Asplund have also calculated the abundance of the first-overtone OH lines using the HM74 model atmosphere and a subset of five lines, resulting in $A_O = 8.79 \pm 0.06$ dex (after normalizing his result with the 15 OH lines). Considering systematic errors of about 0.02 dex, and mainly considering the large statistical errors involved, the results with the HM74 model atmosphere are in reasonable agreement.

Before comparing our results with those obtained with other lines analyzed with 3D hydrodynamical atmospheres, we estimate the total error of our oxygen abundance for the 3D case. The quadratic sum of the observational error (≈ 0.06 dex), the error of the gf -values (≈ 0.03 dex), and a systematic error of (at least) 0.02 dex, results in a total error of $\delta A_O = 0.07$ dex.

4. Comparison with 3D studies

Considering that Kurucz model atmospheres are widely used in the literature, we have also employed a Kurucz solar model to determine oxygen abundances using the [O I], O I and $\Delta v = 0, 1$ OH lines. For comparison purposes, the abundance from these spectral features was also obtained using the <3D> solar model. In short, the equivalent widths and gf -values of the [O I] and the O I 777 nm triplet was obtained from A04 (note that W_λ for the forbidden lines are cleaned from the Ni I and CN blends), and the equivalent widths for the $\Delta v = 1$ and pure rotation OH lines were measured from the WL03 and ATMOS solar atlas, respectively. The gf -values for the molecular lines are from G98, which are essentially identical to the gf -values employed by A04. NLTE corrections for the O I triplet were taken

from A04.

In Table 2 a comparison of our results with those obtained by A04 is shown. For the 3D case we can see that the molecular lines seem to give slightly lower abundances than the [O I] and O I lines. This has been already noted by AP04, who suggested that this difference could signal that the results derived from the infrared OH lines are less reliable than those obtained from the forbidden and permitted lines.

Are these small differences in the abundance obtained from different features due to errors in the transition probabilities? The gf -values of the pure rotation OH lines seem highly reliable. In fact, an accurate dipole moment (1.6676 ± 0.0009 Debye) for $v = 0$, $J = 9/2$, have been measured by Meerts & Dynamus (1973). As the vibration-rotation interaction of the pure rotational lines is very small, an extrapolation of the DMF (using theoretical calculations) for lines with higher J and v seems safe (see e.g. Fig. 2 of Sauval et al. 1984). Goldman et al. (1983) adopted a constant DMF for their analysis of the oxygen abundance in the Sun from the pure rotation OH lines. They made a small correction to the experimental value derived by Meerts & Dynamus (1973), to take into account the higher J values of the solar lines. In Fig. 3a we show the difference between the gf -values derived by G98 and Goldman et al. (1983), as can be seen, neglecting the variation of the DMF results in an error of less than 1%. A comparison between the gf -values obtained from G98 and Goorvitch et. al. (1992) is also shown in Fig. 3a. Goorvitch et al. adopted Nelson's DMF, so the agreement with G98 is not surprising. The error bars shown in Fig. 3a. were estimated from the maximum error that is made if a constant DMF were adopted (for typical solar pure rotation OH lines with $v = 0, 1, 2, 3$). An error of 0.01 dex for the gf -values of the $\Delta v = 0$ sequence is not unreasonable.

The errors for the fundamental ($\Delta v = 1$) OH lines were estimated by N90, as discussed in §3. In Fig. 3b are shown these errors and the difference between the gf -values derived from G98 and N90. In a different approach, G98 made error estimates by making slight modifications to the shape of the experimental DMF by N90. Using these results we obtained the dashed error bars shown in Fig. 3b. The typical error for the gf -values of the $\Delta v = 1$ lines seem to be about 0.035 dex.

In §3 we discussed the errors for the transition probabilities of the $\Delta v = 2$ OH lines, they are shown in Fig. 3c, and are about 0.03 dex.

AP01 states that the uncertainty of the gf -values of the forbidden lines is about 0.02 dex. Lambert (1978) suggested $\log gf = -9.75$ for the 6300 Å line, 0.03 dex lower than the gf value adopted by AP01 and A04, and the NIST database of critically selected transition probabilities suggests $\log gf = -9.78$, 0.03 lower than the value recommended by Lambert

(1978). We adopt an uncertainty of 0.03 dex in the *gf*-value of the forbidden lines. Another important uncertainty in the O abundance derived from the 6300 and 6363 Å [O I] lines is due to blends with Ni I and CN lines. In order to evaluate these uncertainties, we have computed synthetic spectra of the CN lines that are blended with the [O I] lines. The contribution of CN lines is negligible for the 6300.3 Å line, but it is very important for the 6363.7 Å line. As already noted by A04, the main blend is due to the (10,5) Q2 25.5 CN line. Our calculation suggests a similar correction to that proposed by A04 (0.5 mÅ). Fortunately, it is possible to observationally check this result, by measuring the (10,5) Q1 25.5 CN line, which obviously has the same excitation potential and *gf*-value as the Q2 CN line. The Q1 CN line at 6365.0 Å is apparently unblended, but the line is very weak and the continuum is difficult to define. After trying several solar atlases, we found that this line was better defined in the Wallace et al. (1998) FTS solar spectrum at disk center. When a correction to solar flux is made⁶, $W_\lambda = 0.35$ mÅ is obtained⁷, which is lower than the 0.5 mÅ employed by A04. The error in $A_O[6363]$ due to this uncertainty in the CN blend is 0.04 dex. On the other hand, adopting a 20% uncertainty for W_λ (Ni I), results in an error of about 0.03 dex in A_O determined from the 6300 Å line. These errors from the CN and Ni I blends have been considered in column 5 of Table 3.

For the permitted lines, A04 used transition probabilities from the NIST database. The difference between these oscillator strengths and two different calculations given by Biémont et al. (1991) is 0.025 dex, so we adopt 0.03 dex as the error in the *gf*-values of the permitted lines.

The adopted errors are shown in Table 3, where are also shown the statistical uncertainties (σ), the errors due to NLTE effects, and estimates of other errors made in the modeling (see Table 3), as well as the quadratic sum of the errors. The error due to NLTE effects is only important for the O I lines. In particular, for the 777 nm triplet, the NLTE correction is $\Delta \approx -0.21$ dex, but it depends on the empirical correction factor S_H . The NLTE correction could be 0.03 dex lower or higher, if $S_H = 0$ (no collisions with H) or $S_H = 1$ (Drawin-like formula) is adopted, respectively (AP04). Conservatively, we have adopted an NLTE error of 0.04 dex, slightly higher than this 0.03 dex uncertainty, and for the abundance obtained from the permitted lines we will consider the mean abundance obtained by A04 and AP04.

In Fig. 5 we show the oxygen abundances obtained from the different lines in the 3D analysis (Table 2), and the error bars obtained above (Table 3). The recommended solar

⁶A04 used the Kurucz et al. (1984) solar flux atlas, instead of a disk center spectrum

⁷Note that if the true continuum is significantly higher than the local continuum, then this measurement is a lower limit

oxygen abundance by A04 ($A_O = 8.66 \pm 0.05$) is also shown. As can be seen, within the errors, all different spectral features, from the optical to the far infrared, are in good agreement. The weighted-average (using the inverse square of the errors as weight) considering all the lines is only 0.02 dex lower than the value recommended by A04.

5. Summary and Conclusions

A low oxygen abundance of $A_O \approx 8.6$ dex (3D, $\langle 3D \rangle$ and MARCS models) was obtained from extremely weak ($\log (W_\lambda/\lambda) \approx -7.2$) first-overtone vibration-rotation OH lines present in the H band. These lines are about a factor of 5 weaker than the fundamental vibration-rotation OH lines present in the L band of the solar spectrum. The OH lines used in this work are the weakest ones ever used to obtain the oxygen abundance of the Sun (e.g. for $\log (W_\lambda/\lambda) = -7.2$, an optical line at 6000 Å has W_λ just 0.4 mÅ).

The present results support the low solar oxygen abundance recently obtained from other spectral features using 3D hydrodynamical model atmospheres (as summarized in Table 2).

Comparing the results obtained with different spectral features and model atmospheres, we can see that the best agreement with the 3D simulations is obtained with the $\langle 3D \rangle$ model, this is not unexpected, since this model represents the temporal and spatial average of different 3D calculations. As stressed by A04, the $\langle 3D \rangle$ model cannot reproduce all 3D effects, due to the lack of atmospheric inhomogeneities; this can be seen comparing columns $\langle 3D \rangle$ and 3D of Table 2. Note that the first overtone OH lines are the less sensitive of the OH lines to the 3D effects, probably because these lines are formed deeper than the fundamental and pure rotation OH lines.

This new determination of the oxygen abundance in the Sun is consistent with the abundance obtained in B and late O stars (Daflon et al. 2003), solving the problem of the Sun being more oxygen-rich than the ISM. Nevertheless, the depth of the solar convection zone computed with the new solar abundance and OPAL opacities (Bahcall & Pinsonneault 2004) is in conflict with the measured value of the base of the convection zone obtained by helioseismology (Basu & Antia 1997, 2004). Accordingly to Basu & Antia (2004), the problem could be solved with an upward revision of either the solar abundances or the opacity tables. Bahcall et al. (2004a,b) have estimated that an increase of about 10% in the OPAL opacity tables is required to solve the “convective zone problem” and to bring the computed sound speed profile into agreement with helioseismological observations. Recently, Seaton & Badnell (2004) have shown that new calculations from the Opacity Project (OP) result in opacities about 5% larger than those given by OPAL (for temperatures and densities near

the base of the solar convective zone), alleviating the difference between solar models and helioseismology, and bringing support for a low solar oxygen abundance.

I thank the anonymous referee for his valuable suggestions and noting recent pre-prints on helioseismology and OP opacities; M. Asplund for his comments, sending the MARCS solar model and performing 3D calculations; L. Wallace for providing a printed copy of the NSO solar atlas; and J. G. Cohen for her comments. NSO/Kitt Peak FTS data used here were produced by NSF/NOAO. I am grateful for partial support from NSF grant AST-0205951 to J. G. Cohen.

REFERENCES

Allende Prieto, C., Lambert, D.L., Asplund, M. 2001, *ApJ*, 556, L63 (AP01)

Allende Prieto, Asplund, M. & Fabiani Bendicho 2004, *A&A*, in press (astro-ph/0405154) (AP04)

Asplund, M., Gustafsson, B., Kiselman, D., Eriksson, K. 1997, *A&A*, 318, 521

Asplund, M., Grevesse, N., Sauval, A. J., Allende Prieto, C., Kiselman, D. 2004, *A&A* 417, 751 (A04)

Bahcall J. N. & Pinsonneault M. 2004, *PRL* 92, 121301

Bahcall J. N., Basu S., Pinsonneault M., Serenelli A. M. 2004a, *ApJ*, submitted, astro-ph/0407060

Bahcall J. N., Serenelli A. M. & Pinsonneault M. 2004b, *ApJ*, submitted, astro-ph/0403604

Basu, S., Antia, H. M. 2004, *ApJ*, 606, L85

Basu, S., Antia, H. M. 1997, *MNRAS*, 287, 189

Biemont, E., Hibbert, A., Godefroid, M., Vaeck, N., Fawcett, B. C. 1991, *ApJ*, 375, 818

Bonnell, J. T. & Bell, R. A. 1993, *MNRAS*, 264, 319

Castelli F. & Kurucz R. L. 2004, IAU Symp. 123, Modeling of Stellar Atmospheres, eds. N. Piskunov et al. 2003, poster A20

Cayrel, R. 1988, IAU Symp. 132, eds. R. Cayrel, G. Cayrel de Strobel, M. Spite, (Dordrecht: Kluwer), 345

Daflon, S., Cunha, K., Smith, V. V., Butler, K. 2003, *A&A*, 399, 525

Goldman A., Shoenfeld W. G., Goorvitch D., et al. 1998, *JQSRT*, 59 453 (G98)

Goldman, A., Murcray, D. G., Lambert, D. L., Dominy, J. F. 1983, MNRAS, 203, 767

Goorvitch, D., Goldman, A., Dothe, H., Tipping, R. H., Chackerian, C., Jr. 1992, JGR, 97, 20771

Grevesse, N. & Sauval, A.J., 1998, SSRv, 85, 161

Grevesse, N., Sauval, A.J. & Dishoeck E. F. 1984, A&A, 141, 10

Hinkle, K. H. & Lambert, D. L. 1975, MNRAS, 170, 447

Holtzclaw K. W., Person J. C. & Green B. D. 1993, JQSRT, 49, 223.

Holweger, H. & Müller, E. A., 1974, Sol. Phys. 39, 19 (HM74)

Huber K. P. & Herzberg G. 1979, Constants of Diatomic Molecules, Van Nostrand, New York

Lambert, D. L. 1978, MNRAS, 182, 249

Meléndez, J. & Barbuy, B. 1999, ApJS, 124, 527

Meléndez, J., Barbuy, B. & Spite, F. 2001, ApJ, 556, 858

Meléndez, J., Barbuy, B., Bica, E. et al. 2003, A&A, 411, 417

Meerts, W. L. & Dynamus, A. 1973, Chem. Phys. Lett., 23, 45

Meyer, D. M., Jura, M., Hawkins, I., Cardelli, J. A. 1994, ApJ, L437

Mies F. H. 1974, J. Molec. Spectrosc. 53, 150

Nelson D. D. Jr., Schiffman A., Nesbitt D. J., Orlando J. J., Burkholder J. B. 1990, J. Chem. Phys., 93, 7003 (N90)

Norris, J.; Ryan, S. G. & Beers T. C. 2001, ApJ, 561, 1034

Sauval, A.J., Grevesse, N., Brault, J. M., Stokes, G. M. & Zander R. 1984, ApJ, 282, 330

Seaton, M. J. & Badnell, N. R. 2004, MNRAS, submitted (astro-ph/0404437)

Sneden, C. 1973, Ph.D. thesis, University of Texas

Turck-Chize, S. Couvidat, S., Piau, L. et al. 2004, PRL, submitted (astro-ph/0407176)

Wallace, L., Hinkle K, & Livingston W. 1998, An Atlas of the Spectrum of the Solar Photosphere from 13500 to 28000 cm $^{-1}$ (3570 to 7405 Å), NSO Tech. Rep. 98-001, Tucson, AZ

Wallace, L. & Livingston W. 2003, An Atlas of the Solar Spectrum in the Infrared from 1850 to 9000 cm $^{-1}$, revised ed., NSO Tech. Rep. 03-001, Tucson, AZ (WL03)

Wielen, R., Fuchs, B., Dettbarn, C. 1996, A&A, 314, 438

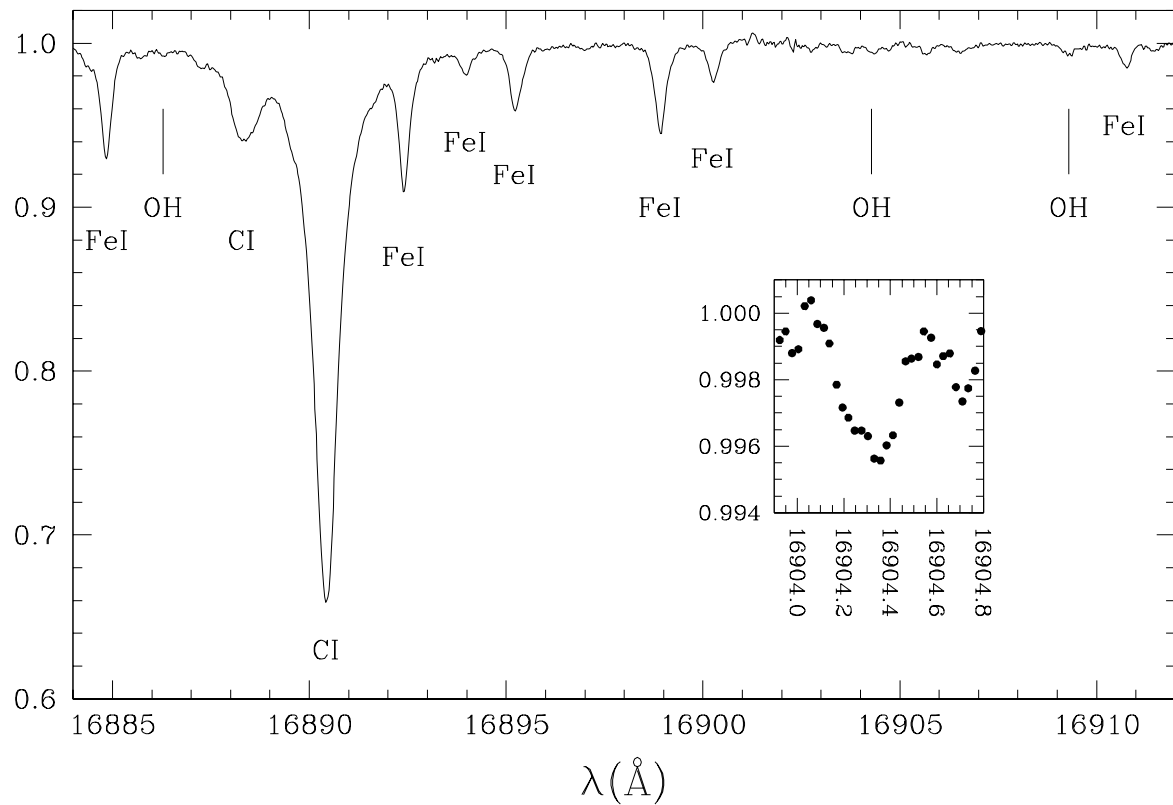


Fig. 1.— Observed solar spectrum (WL03) around $1.69 \mu\text{m}$. The vertical lines indicate three OH lines used in this work. The strongest atomic features are identified. The profile of the OH line at 16904.3 \AA is shown in the inset, where only the upper 0.7 % of the spectrum is plotted.

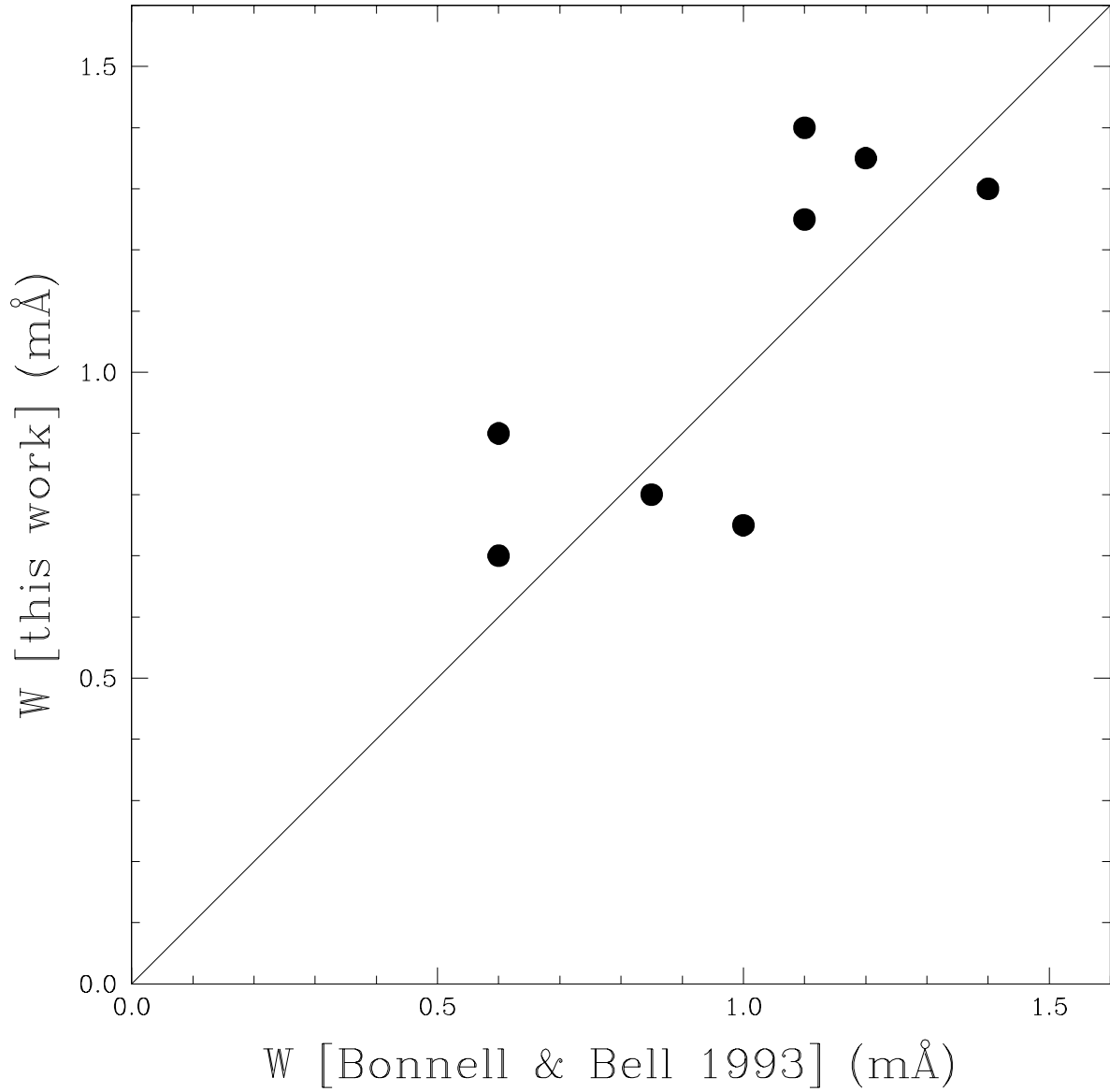


Fig. 2.— Comparison between our W_λ measurements and those by Bonnell & Bell (1993). The line depicts perfect agreement.

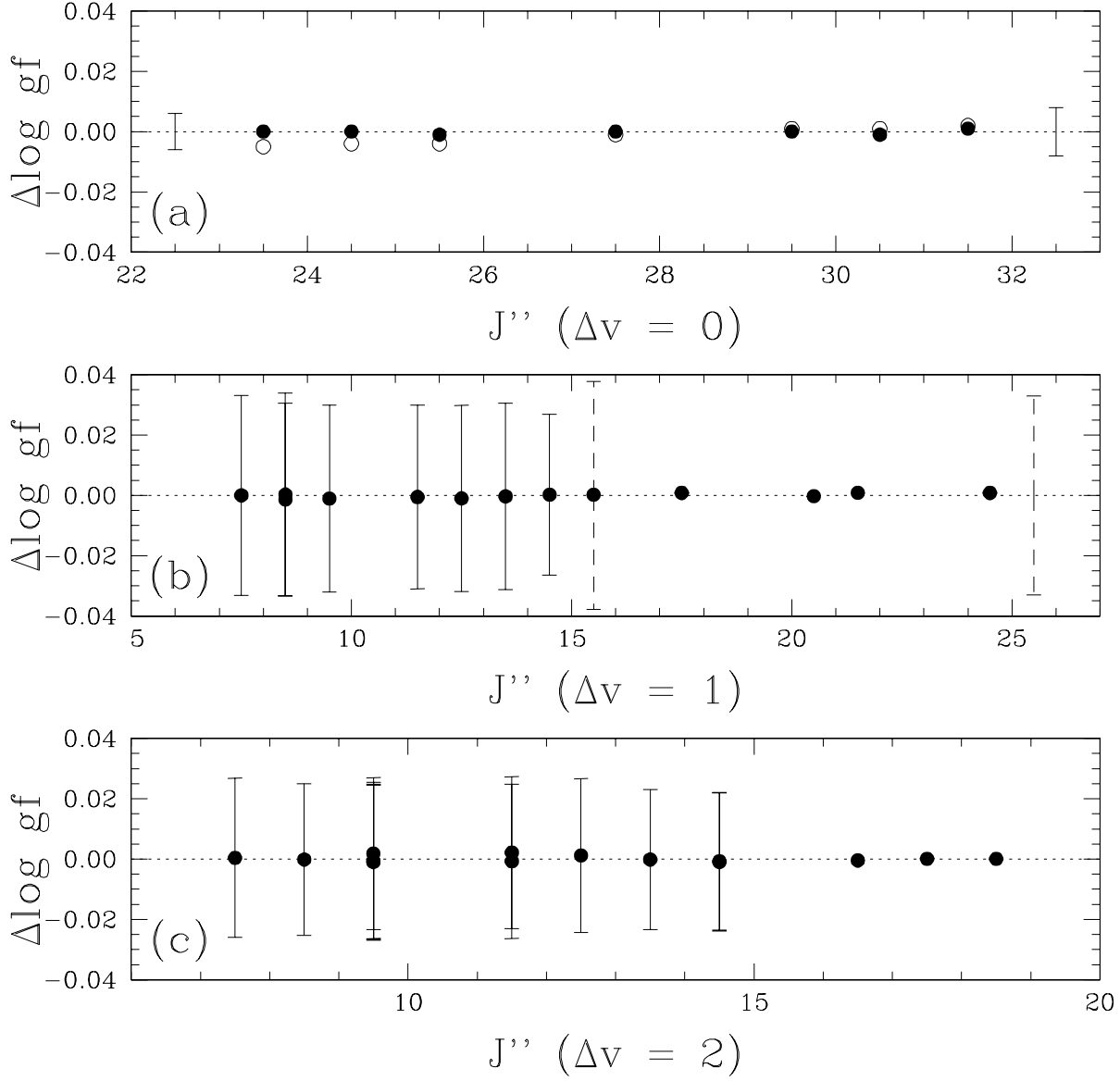


Fig. 3.— Differences between the g_f -values of infrared OH lines calculated by G98 and (a) Goorvitch et al. (1992) (filled circles) and Goldman et al. (1983) (open circles); (b) and (c) N90 (filled circles). The error bars given in (a) were obtained supposing that the DMF is constant. The solid error bars in (b) and (c) were estimated by N90 taken into account the error of its experimental DMF. The dashed error bars in (b) were estimated from slight variations to the Nelson's DMF, as given in the last column of Table 3 by G98.

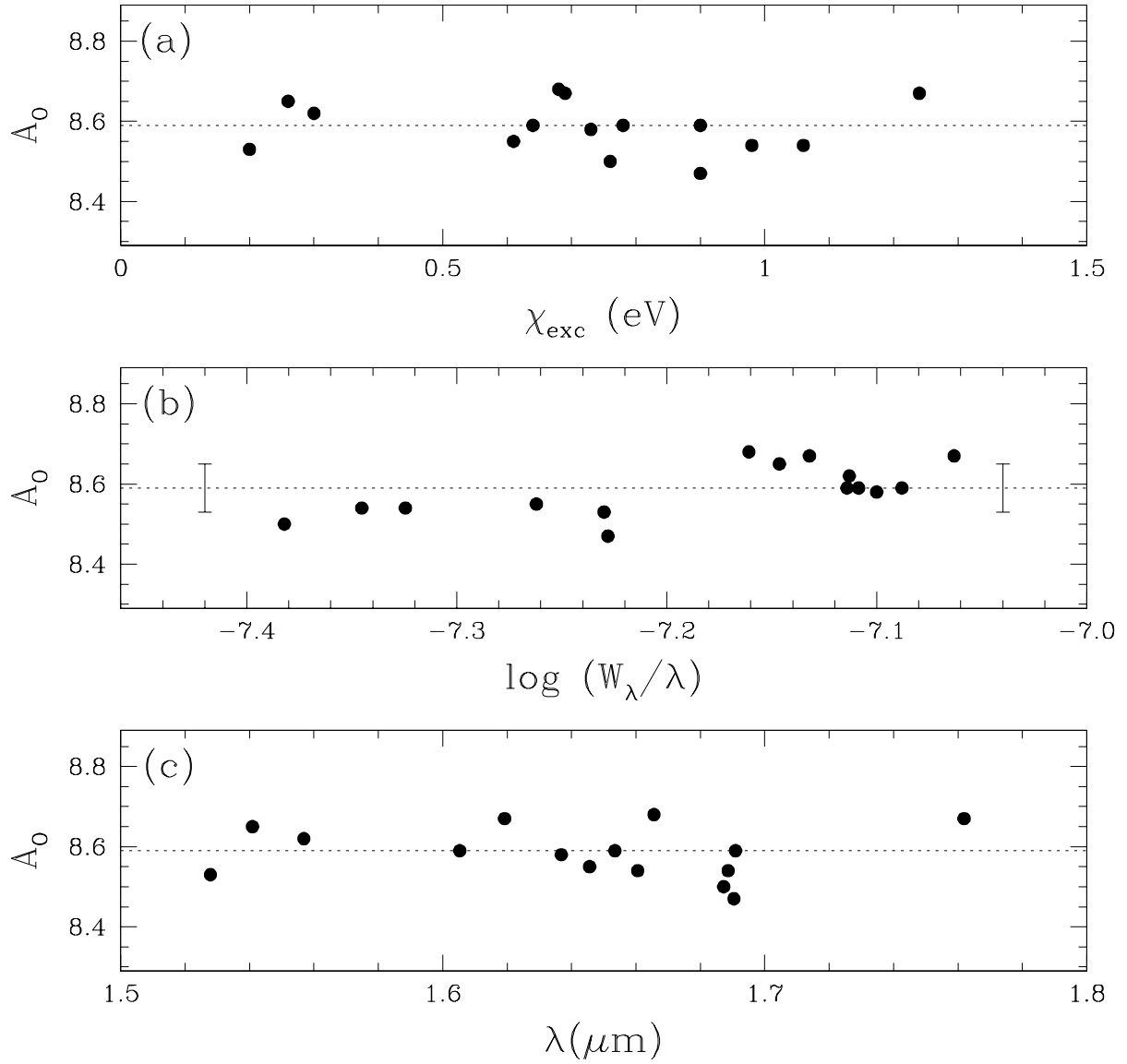


Fig. 4.— Solar oxygen abundances obtained with the <3D> model and first overtone infrared OH lines (filled circles) vs. (a) excitation potential, (b) W_λ/λ , and (c) wavelength. The mean abundance ($A_O = 8.59$ dex) is shown by dotted lines, and the σ (0.06 dex) error bar is shown in the middle panel.

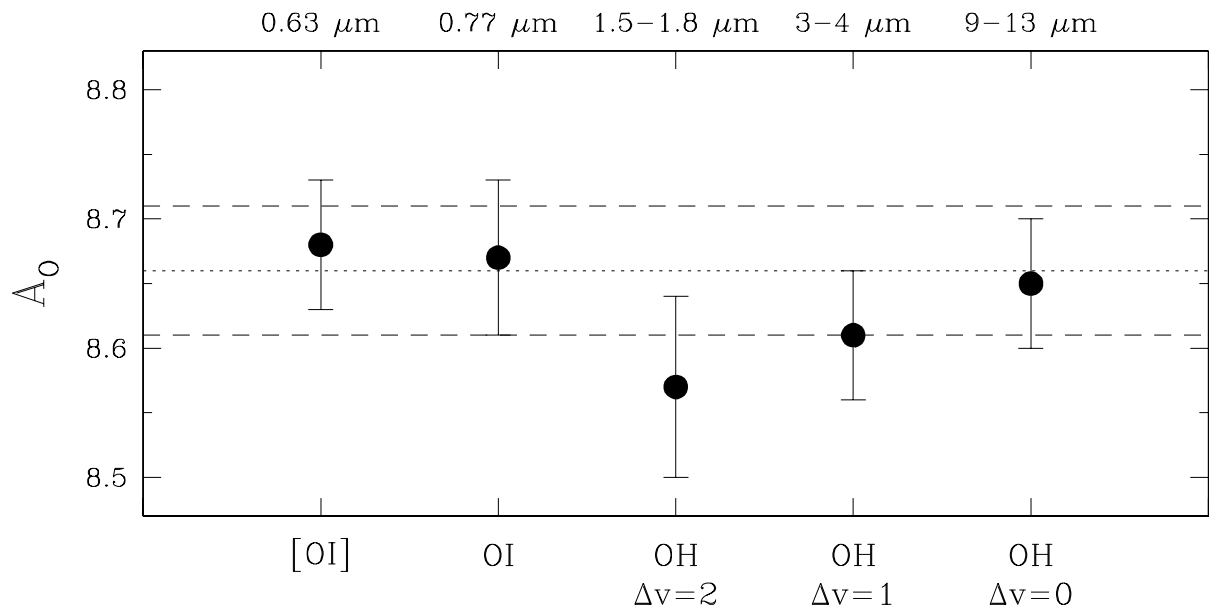


Fig. 5.— Solar oxygen abundance derived from different lines in 3D analyses (Table 2). The error bars are from Table 3. The recommended value given by A_O4 ($A_O = 8.66 \pm 0.05$ dex) is shown by the dotted and dashed lines.

Table 1. Equivalent widths of OH lines

λ^a (Å)	ID ^b	χ_{exc} (eV)	$\log gf$ (dex)	W_λ (mÅ)
15278.52	(2,0) P1e 9.5	0.205	−5.382	0.9
15409.17	(2,0) P2e 9.5	0.255	−5.365	1.1
15568.78	(2,0) P1e 11.5	0.299	−5.269	1.2
16052.76	(3,1) P1e 9.5	0.639	−4.910	1.25
16192.13	(3,1) P2e 9.5	0.688	−4.893	1.4
16368.13	(3,1) P1f 11.5	0.731	−4.797	1.3
16456.04	(2,0) P1f 16.5	0.609	−5.048	0.9
16534.58	(3,1) P1e 12.5	0.782	−4.746	1.35
16605.46 ^c	(4,2) P1e 7.5	0.982	−4.755	0.75
16655.99	(2,0) P1e 17.5	0.682	−5.010	1.15
16872.28 ^c	(2,0) P1e 18.5	0.759	−4.975	0.7
16886.28	(4,2) P2e 8.5	1.059	−4.662	0.8
16904.28	(3,1) P1e 14.5	0.897	−4.654	1.0
16909.29	(3,1) P1f 14.5	0.898	−4.654	1.3
17618.89	(4,2) P1e 13.5	1.244	−4.403	1.3

^aidentifications in the solar spectrum by WL03

^b(v',v'') branch J''

^clines identified in this work

Table 2. Solar oxygen abundance from different spectral features and model atmospheres.

lines	3D	HM74	MARCS	<3D>	Kurucz
[O I] ^a	8.68 ± 0.01	8.76 ± 0.02	8.72 ± 0.01	8.75 ± 0.01	8.79 ± 0.01
O I ^a	$8.67^c \pm 0.02$	8.64 ± 0.08	8.72 ± 0.03	8.68 ± 0.03	8.67 ± 0.01
OH ($\Delta v = 0$) ^a	8.65 ± 0.02	8.82 ± 0.01	8.83 ± 0.03	$8.74^d \pm 0.05$	$8.80^e \pm 0.06$
OH ($\Delta v = 1$) ^a	8.61 ± 0.03	8.87 ± 0.03	8.74 ± 0.03	8.69 ± 0.06	8.82 ± 0.05
OH ($\Delta v = 2$) ^b	8.57 ± 0.06	8.80 ± 0.06	8.61 ± 0.06	8.59 ± 0.06	8.71 ± 0.06

Note. — The quoted uncertainties are only the σ (line-to-line scatter)

^aResults from A04 for the 3D, HM74 and MARCS models, and abundances obtained in this work for the <3D> and Kurucz models

^bThis work, except for the 3D case. The 3D calculations were performed by M. Asplund, who obtained 8.58 ± 0.05 for 5 OH lines of the $\Delta v = 2$ sequence, using this result we found $A_O = 8.57 \pm 0.06$ for the 15 OH lines

^cThis is the mean of the abundance obtained by A04 and AP04

^d $A_O = 8.75 \pm 0.03$ dex is obtained when only lines with $W_\lambda = 15\text{-}100 \text{ m}\text{\AA}$ are employed

^e $A_O = 8.82 \pm 0.03$ dex for the lines with $W_\lambda = 15\text{-}100 \text{ m}\text{\AA}$

Table 3. Errors in the oxygen abundance (dex)

lines	σ^a	gfs	NLTE	others ^b	total
[O I]	0.01	0.03	0.00	0.04	0.05
O I	0.02	0.03	0.04	0.02	0.06
OH ($\Delta v = 0$)	0.01	0.01	0.00	0.05	0.05
OH ($\Delta v = 1$)	0.03	0.04	0.00	0.02	0.05
OH ($\Delta v = 2$)	0.06	0.03	0.00	0.02	0.07

^aline-to-line scatter

^bminimum uncertainties in the 3D modeling, due to systematic errors in the continuum opacities, partition functions, etc. For the [O I] lines errors due to blends with Ni I and CN lines are considered. A higher error for the pure rotation lines was adopted because the 3D modeling is less successful for these lines (see Fig. 10 of A04)